AN EX VIVO MODEL OF OXIDATIVE STRESS INDUCED TRABECULAR MESHWORK DYSFUNCTION FOR GLAUCOMA RESEARCH

A Thesis
Presented to
The Academic Faculty

by

Becky Hardie

In Partial Fulfillment
of the Requirements for the Degree
Bachelor of Science in Biomedical Engineering in the
Wallace H. Coulter Department of Biomedical Engineering at the
Georgia Institute of Technology

Georgia Institute of Technology
May 2019

An *Ex Vivo* Model of Oxidative Stress Induced Trabecular Meshwork Dysfunction for Glaucoma Research

Approved by:

Dr. C. Ross Ethier, Advisor
Wallace H. Coulter Department of Biomedical Engineering
Georgia Institute of Technology

Dr. Lisa Schildmeyer
Wallace H. Coulter Department of Biomedical Engineering
Georgia Institute of Technology

Date Approved: May 2019

TABLE OF CONTENTS

ACKNOWLEDGMENTS

I wish to thank Dr. C. Ross Ethier, Dr. Eric Snider, and the rest of the Ethier lab for their invaluable support and mentorship.

LIST OF FIGURES

LIST OF SYMBOLS AND ABBREVIATIONS

ANOVA……..……..Analysis of variance

DMEM……..……Dulbecco's modified Eagle's medium

DNA……..……..Deoxyribonucleic acid

ECM……..…….Extracellular matrix

EDTA…….…….Ethylenediaminetetraacetic acid

FBS…….…….Fetal bovine serum

H_2O_2……..……..Hydrogen peroxide

HBSS……..……Hank's balanced salt solution

IOP…….Intraocular pressure

MFI…….……..Median fluorescent intensity

MIP……Maximum intensity projection

MSC…….Mesenchymal stem cell

PBS……..…….Phosphate buffered saline

POAG…….Primary open angle glaucoma

pTM……...……..Porcine trabecular meshwork

TM……...……Trabecular meshwork

SUMMARY

Affecting more than 70 million people worldwide, glaucoma is one of the leading causes of vision loss and blindness. Although the exact origins of glaucoma are still unknown, elevated intraocular pressure is a well-established risk factor. Intraocular pressure is primarily regulated by the trabecular meshwork, a tissue located in the anterior segment of the eye which drains aqueous humor. The cellularity of the trabecular meshwork is shown to be significantly reduced in glaucoma. This loss of cellularity presumably leads to reduced trabecular meshwork function and increased outflow resistance, which in turn leads to elevated intraocular pressure. In order to assess regenerative medicine therapies for glaucoma, the damage to the trabecular meshwork observed in glaucoma must be properly modeled. This study demonstrates that oxidative stress caused by hydrogen peroxide can reduce trabecular meshwork cellularity to glaucomatous levels in a porcine anterior chamber organ culture model. The diminished trabecular meshwork cellularity resulted in a loss of intraocular pressure homeostasis and the hydrogen peroxide treatment did not permanently damage the trabecular meshwork. This porcine organ culture model provides a platform for evaluating trabecular meshwork regenerative medicine therapies that could be possibly used to treat glaucoma.

1 INTRODUCTION

Glaucoma is one of the leading causes of vision loss and blindness and the number of affected individuals is expected to continue to grow with an aging population (Quigley & Broman, 2006; Weinreb et al., 2014). There are several types of glaucoma; however, most are characterized by damage to the optic nerve resulting in vision loss (Weih et al., 2001). Primary open-angle glaucoma (POAG), which causes irreversible blindness, is the most common form of glaucoma, representing approximately 74% of cases worldwide (Quigley & Broman, 2006). While the complete pathophysiology of glaucoma is not understood, patients with POAG have elevated intraocular pressure (IOP) leading to optic nerve head damage (Weinreb et al., 2014).

IOP is largely determined by the relative rates of production and drainage of aqueous humor in the anterior chamber of the eye. Aqueous humor is secreted from the ciliary body and drains through the TM into Schlemm's canal. Since aqueous humor production has been found to be independent of IOP, increased IOP is usually due to decreased outflow through the TM and Schlemm's canal (Acott et al., 2014; Brubaker, 1970, 1991). Decreased outflow of aqueous humor is linked to increased resistance and around 75% of conventional outflow resistance is localized to the TM, thus the TM is thought to be particularly relevant in glaucoma (Acott & Kelley, 2008).

The cellularity of the TM has been shown to significantly decrease with age, with up to 60% loss by age 80 (Alvarado et al., 1981; Grierson & Howes, 1987). An even greater reduction in cellularity, approximately an additional 30% decrease, has been noted in glaucomatous eyes compared to age-matched, healthy eyes (Alvarado et al., 1984; Liton et al., 2005). The decreased TM cellularity presumably leads to diminished function and increased outflow resistance and subsequent elevated IOP.

Therapies focusing on restoring TM cellularity and function using regenerative medicine may be beneficial for POAG patients. In order to assess stem cell therapies for restoring the TM in glaucomatous eyes, a glaucoma model that displays this reduced cellularity and loss of TM function is needed. Ideally, the method that causes TM dysfunction would not permanently damage the TM or alter the aqueous humor outflow pathways in a non-physiological manner. Most current glaucoma models are focused on studying optic neuropathy due to elevated IOP and thus damage the TM in the process of elevating IOP (Gaasterland & Kupfer, 1974; Ishikawa et al., 2015; Morrison et al., 1997; Shareef et al., 1995; Weber & Zelenak, 2001).

There are a few models that display reduced TM cellularity without severe and irreversible TM damage, most notably those of Zhang *et al.*, Senatorov *et al.*, and Abu-Hassan *et al.*. Zhang *et al.* ablated the TM with a cytotoxic vector; however, their model demonstrated reduced IOP after TM damage. Senatorov *et al.* used a mouse model and expressed mutant myocilin which led to elevated IOP as in glaucoma. However, since mutations in myocilin are only linked with 3-4% of POAG cases, Senatorov *et al.*'s method may not translate directly to other POAG varieties (Tamm, 2002). Abu-Hassan *et al.* used saponin, a plant-derived detergent, to reduce TM cellularity and alter IOP homeostasis in organ-cultured human eyes. Unfortunately, their method was unsuitable for more readily available porcine or bovine tissue (Snider, 2018).

Many studies on glaucoma and other ocular diseases use anterior chamber organ culture models to study the eye. Anterior chamber organ culture is a well-established method that has been shown to be suitable for maintaining monkey, porcine, bovine, and human eyes for multiple weeks, *ex vivo*, under physiological IOP (Bachmann et al., 2006; Bhattacharya et al., 2009; Erickson-Lamy et al., 1991; Johnson & Tschumper, 1987, 1989; Mao et al., 2011). Since human organ culture models have been shown to be effective, the most obvious method for assessing regenerative medicine therapies is using glaucomatous human tissue. However, low availability and high cost make relying on human eyes impractical for many experiments. Additionally, most available human glaucomatous eyes have undergone some sort of glaucoma treatment, impacting the ability to consistently evaluate potential therapies. As a result, there is a demand for a porcine or bovine organ culture model that demonstrates reduced TM cellularity and diminished TM function along with elevated IOP.

In this study, oxidative stress is used to cause TM damage and dysfunction. Evidence suggests that the TM is subjected to oxidative stress during glaucoma progression, leading to DNA, mitochondrial, and extracellular matrix (ECM) damage (Clopton & Saltman, 1995; Knepper et al., 1996; Saccà et al., 2005; Tanito et al., 2016; Yu et al., 2008; Zhao et al., 2016). In addition, the TM has been found to be more susceptible to damage from oxidative stress than other anterior tissues such as the cornea (Izzotti et al., 2009). Consequently, oxidative stress is an attractive option for recreating the TM dysfunction seen in glaucoma. Here, we show that hydrogen peroxide (H_2O_2) can be used to reduce TM cellularity in porcine eyes, which leads to tissue dysfunction and a subsequent loss in IOP homeostasis. This organ culture model offers an improved platform to assess stem cell therapies for restoring function to the TM in glaucoma.

2 MATERIALS AND METHODS

2.1 Cell Sourcing

Porcine trabecular meshwork (pTM) cells were previously isolated and characterized from porcine tissue from a slaughterhouse (Holifield Farms, Covington, GA) using established methods (as previously described (Stamer et al., 1995)).

2.2 In Vitro Exposure to Hydrogen Peroxide

Viability assessments (see section 2.3.1) and functional experiments (see sections 2.3.2 – 2.3.4) were conducted after pTM cells had time to deposit ECM and proliferate (Snider, 2018). Cells were plated in 10% FBS DMEM at 10,000 cell/cm^2 and incubated for at least 48 hours at 37°C. TM cell media was aspirated, and adherent cells were washed with phosphate-buffered saline (PBS). Commercially-available hydrogen peroxide (H_2O_2, 3% w/v), obtained fresh every 3 months, was 0.22μm sterile filtered and prepared at specified concentrations in organ culture media (serum-free DMEM supplemented with 2mM L-glutamine and 1x penicillin, streptomycin, and amphotericin). After treatment with H_2O_2, cells were incubated for 1 hour at 37°C, 5% CO_2. H_2O_2 media was then removed, cells were washed once in PBS, and TM cell media was added for further cell culture.

2.3 pTM Cell Characterization After Hydrogen Peroxide Treatment

2.3.1 Cellular Viability Assessment *In Vitro*

To determine pTM cellular viability, dead, adherent cells were stained with propidium iodide in PBS after H_2O_2 treatment in 24 well plates. Cells were incubated for 5 minutes at 37°C after which propidium iodide was replaced with 0.05% Trypsin-EDTA (w/v) for 5 minutes to detach cells from the plate. TM cell media was added to prevent further trypsin activity, cell suspensions were collected in deep well 96 well plates (Corning), and samples were processed with flow cytometry (Attune NxT). Viability following H_2O_2 treatment was determined by comparing living, unstained cell counts in the treatment groups to untreated, control cell counts. Viability was assessed immediately, 24 hours, and 48 hours after H_2O_2 treatment (Snider, 2018).

2.3.2 Metabolic Activity Assessment *In Vitro*

Following H_2O_2 treatment in 6 well plates, pTM cells were incubated at 37℃ for 24 hours before being re-plated in Hanks' balanced salt solution (HBSS) supplemented with 5% FBS and 2mM L-glutamine. Assessment of the effect of oxidative stress on metabolic activity was performed in 96 well plates with cells seeded at 10,000 cells/cm^2. After a further 24 hours incubation period, 10% Alamar blue (resazurin) in TM cell media (w/v) was added to each sample (O'Brien et al., 2000). Plates were then incubated in a 5% CO_2 environment for at least 2 hours with the increase in Alamar blue fluorescence detected with a plate reader (Cytation 3, Bio-Tek) taking readings (excitation wavelength 545nm, emission wavelength 590nm) every 10 minutes (Snider, 2018). Alamar blue fluorescence was plotted versus time for each cell sample, the slope of the linear region of the plot was found, and slopes were compared between H_2O_2 treated and untreated, control samples to determine the effect of H_2O_2 treatment on the metabolic activity of TM cells (Snider, 2018).

2.3.3 Phagocytic Activity Assessment *In Vitro*

In vivo, TM cells have been shown to remove particulate matter and cellular debris from the aqueous humor to prevent clogging the meshwork (Buller et al., 1990; Sherwood & Richardson, 1988). To quantify this phagocytic activity, pHrodo *e. coli* BioParticles (Life Technologies) were used following previously described methods (Gagen et al., 2013; Snider et al., 2018). After H_2O_2 treatment in 6 well plates and an incubation period of 24 hours, pTM cells were re-plated on 96 well plates at 50,000 cells/cm^2. Cells were allowed to attach overnight, in HBSS supplemented with 5% FBS and 2mM L-glutamine, before assessing their phagocytic activity.

pHrodo particles (2 million cells/vial) were reconstituted in HBSS media, sonicated for 5 minutes, and added to cell samples. Cell samples were incubated for 4 hours at 37℃, after which HBSS media was removed (Snider, 2018). Adherent cells were detached with 0.05% Trypsin-EDTA and cell suspensions were collected in 96 well plates and analyzed with 100µL/min flow cytometry (Attune NxT). Unstained median fluorescent intensity (MFI) values were subtracted from MFI values measured in phagocytically-challenged samples. Ratios of MFI values in H_2O_2 treated cells to MFI values in untreated, control cells were calculated to determine the effect of oxidative stress on pTM phagocytic activity (Snider, 2018).

2.3.4 Cellular Contractility Assessment *In Vitro*

TM cells are known to be contractile (Dismuke et al., 2014), thus the effect of oxidative stress on cell contractility was determined using a collagen gel contraction assay. pTM cells were resuspended in serum-free DMEM at 9 x 10^5 cells/mL, 24 hours after H_2O_2 treatment. Collagen type I (3mg/mL, 1% [v/v] acetic acid, calf skin, MP Biomedical) was added to cell suspensions at a 1:2 volume ratio (collagen:cells), followed immediately by a pre-titrated volume of 0.1M sodium hydroxide. Collagen gels (1mg/mL, 6 x 10^5 cells/mL) were cast in 48 well plates with 240µL of solution per well. After gelation occurred, 240µL of serum-free media was added to provide nutrients while minimizing proliferation (Snider, 2018). Gels were released from the walls of the 48 well plate 24 hours later and incubated for an additional 24 hours to allow for the pTM cells to contract and reach steady state. The size of each gel was determined with images taken immediately following release from the well wall and after 24-hour incubation (ChemiDoc MP, Bio-Rad). Gel area was quantified using ImageJ and the magnitude of contraction was determined by comparing the initial gel size with the steady-state, contracted size. Percent gel contraction was compared between H_2O_2 treated and untreated, control samples (Snider, 2018).

2.4 Organ Culture Setup

2.4.1 Porcine Eye Preparation and Dissection

Fresh porcine eyes were obtained from a slaughterhouse (Holifield Farms, Covington, GA) within 6-8 hours of enucleation. Eyes were dissected to isolate the anterior chamber using previously described methods (Bachmann et al., 2006; Bhattacharya et al., 2009). Briefly, connective tissue was removed and whole eyes were soaked in Betadine solution (Purdue Pharma) for 5 minutes (Snider, 2018). Eyes were then washed in PBS with 5x penicillin, 5x streptomycin, and 1x amphotericin under a sterile laminar flow hood and stored in the aforementioned antibiotic PBS solution until dissection. A razor blade was used to cut the eyes in half, isolating the front half of the eye. The vitreous humor and lens were removed and the iris was cut back radially to the iris root and pectinate ligaments to reveal the TM (Snider, 2018). Any remaining non-TM tissue was carefully removed using Vannas microscissors (World Precision Instruments) and the dissected anterior segments were placed in antibiotic PBS.

2.4.2 Porcine Anterior Segment Organ Culture

Custom-built organ culture dishes were designed to clamp the front half of the eye and create sealed hemispheres (Figure 1a and b). Organ culture dishes with dissected porcine anterior segments were kept in a sterile 37°C humidified incubator. Eyes were perfused with organ culture media at 2.5µL/min and the pressure in each eye was measured every 60 seconds (142pc01g, Honeywell). Organ culture eyes were stabilized for at least 48 hours before treatment and the outflow facility (a ratio between perfusion flow rate and IOP) was monitored in LabView. All eyes which did not achieve a steady outflow facility of between 0.125 and 0.45µL/min/mmHg were removed before treatment (Figure 1c). This range of outflow facility corresponds to pressures of ~6mmHg to 20mmHg, representing normal porcine IOPs (Snider, 2018).

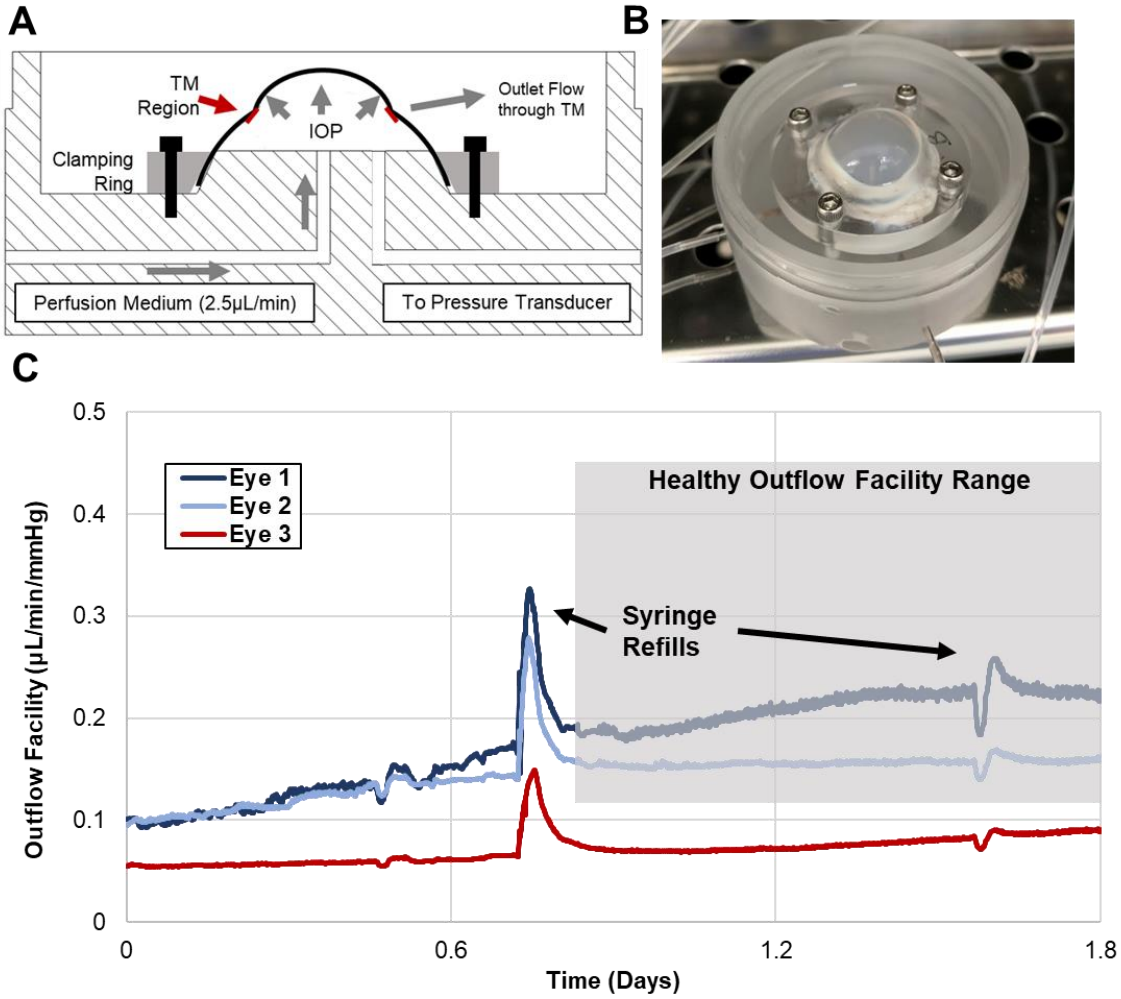

Figure 1. Porcine Anterior Chamber Organ Culture Setup. (A) Schematic of an organ culture dish and clamped porcine anterior segment with the TM location and perfusion pathways shown. (B) Clamped porcine anterior segment in an organ culture dish after 10 days of perfusion and incubation. (C) Representative graph of outflow facility for 3 organ culture eyes, illustrating pressure stabilization and healthy outflow range.

2.4.3 Hydrogen Peroxide Treatment in Organ Culture

After the 48-hour stabilization period, porcine organ culture eyes were perfused with 4.5mM H_2O_2 in organ culture media for 1 hour. To prevent dilution of the H_2O_2 and rapidly create oxidative stress, the flow rate was increased from 2.5µL/min to 2.5mL/min. While the flow rate was increased, organ culture dishes were open to hydrostatic reservoirs to maintain pressure and allow for media outflow. After approximately 10mL of the H_2O_2 treatment media had been perfused, the flow rate was returned to 2.5µL/min and the valve to the hydrostatic reservoir was closed. After the 1-hour H_2O_2 treatment period, fresh organ culture media was perfused into the anterior segment using the same flow rate increase procedure. Eyes were perfused with organ culture media at 2.5µL/min for an additional 24 hours post-treatment to allow for the increased oxidative stress to take effect in the TM. The untreated, control eyes underwent the same flow rate increases as the treated anterior segments, however, no H_2O_2 was added to the perfusion media (Snider, 2018).

2.5 Organ Culture Characterization

2.5.1 IOP Homeostasis Challenge

A “2x flow challenge” was created for the organ culture eyes after the post-treatment stabilization period. The perfusion flow rate was doubled to 5µL/min for 72 hours to create an increase in pressure (Figure 2). A similar pressure challenge in human organ culture eyes has shown higher facility and the eventual return to IOP homeostasis in healthy, normal eyes. This adaptive response was absent or severely diminish in glaucomatous eyes (Abu-Hassan et al., 2015; Snider, 2018). It is thought that TM remodeling plays an important role in the maintenance of IOP homeostasis and it is expected that the H_2O_2 treated anterior segments with damaged TMs will not adapt in response to the increased flow and pressure (Snider, 2018).

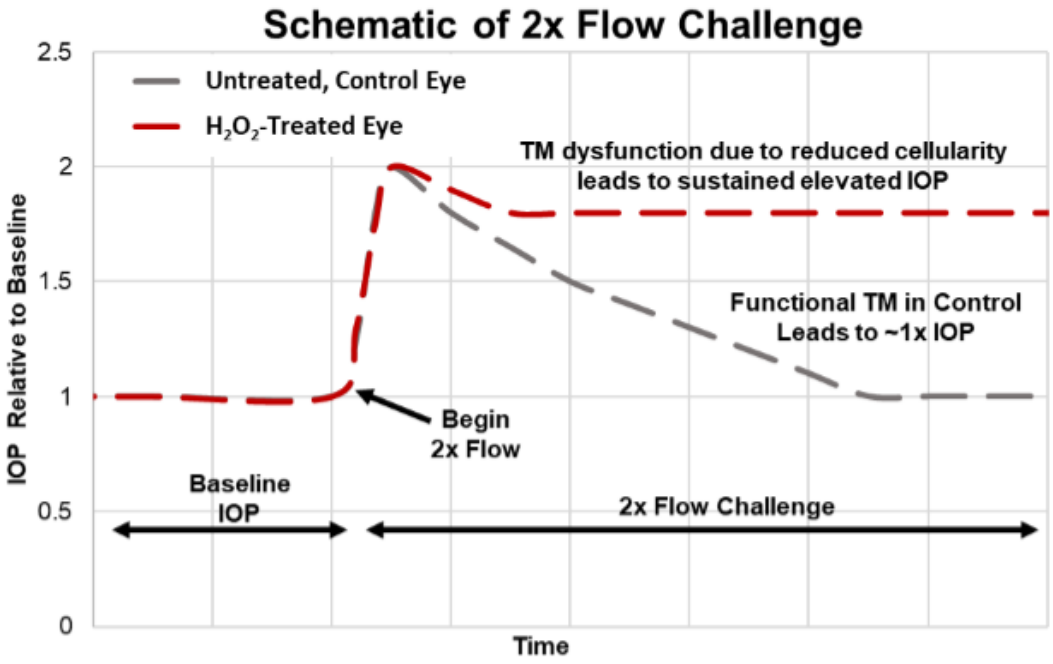

Figure 2. Schematic of 2 Flow Challenge for Organ Culture Anterior Segments. Baseline IOP was established following a stabilization period post-treatment after which the perfusion flow rate was doubled to create a "2x flow challenge". Initially, IOP in both control and H_2O_2-treated eyes spikes. It is expected that the undamaged, functional TM in untreated, control eyes will remodel in response to the increased pressure and adapt to return IOP to the baseline. IOP is expected to remain elevated due to TM dysfunction in the H_2O_2-treated anterior segments.

2.5.2 Cellular Viability Assessment *Ex Vivo*

Cellular viability of the TM in organ culture anterior segments was determined following the post-treatment stabilization period. Eyes were removed from organ culture dishes and washed in PBS. Live-dead staining was performed by incubating the anterior segments in 2µM calcein-AM and 4µM ethidium homodimer-1 for 30 minutes. Tissue samples were imaged *en face* by confocal microscopy (LSM 700, Carl-Zeiss) and captured as tile scans of z-stacks at 50x magnification. Maximum intensity projections (MIPs) were created from z-stacks for image quantification (Snider, 2018).

The location of the TM in the tissue sample was determined using brightfield overlays which clearly indicated the location of the cornea. The TM region was defined as a 1mm band around the corneal margin. Within the TM region, the average fluorescent intensities for live (calcein-AM) and dead (ethidium homodimer-1) staining was determined in ImageJ using the

MIPs. This average fluorescent intensity was compared between untreated, control eyes and H_2O_2 treated eyes to determine the effect of oxidative stress on TM cellular viability in organ culture (Snider, 2018).

2.6 Statistical Analysis

For *in vitro* experiments, at least 4 technical replicates of at least 2 pTM cell lines were assessed. For *ex vivo* organ culture experiments, control and treatment groups contained at least 6 eyes each. Analysis of variance (ANOVA, post hoc Tukey test) was used to determine statistical significance ($p < 0.05$) in the difference between untreated, control and H_2O_2 treated groups. A paired Student's t-test ($p < 0.05$) was used to determine differences in baseline IOP for 2x flow challenge organ culture experiments.

3 RESULTS

3.1 Effect of Hydrogen Peroxide on pTM Cellular Viability In Vitro

Isolated pTM cells were treated with various H_2O_2 concentrations for 1 hour after which cellular viability was determined using flow cytometry. H_2O_2 concentration and pTM cell viability had a negative, linear correlation (Figure 2a). However, further investigation revealed that cellular viability continued to decrease after the initial 1-hour H_2O_2 treatment. pTM cell viability was thus assessed immediately and at 24 and 48 hours after treatment, with the cells for the 24- and 48-hour time points kept in serum-free media post-treatment. Viability 24 and 48 hours after 2mM H_2O_2 treatment was similar for multiple pTM cell lines (Figure 2b). Additionally, across three pTM cell lines, cellular viability was similar following 1-hour treatment with 2mM H_2O_2 and a 24-hour stabilization period (Figure 2c). We conclude that treatment of pTM cells with H_2O_2 consistently produces a concentration-dependent reduction in cellularity (Snider, 2018).

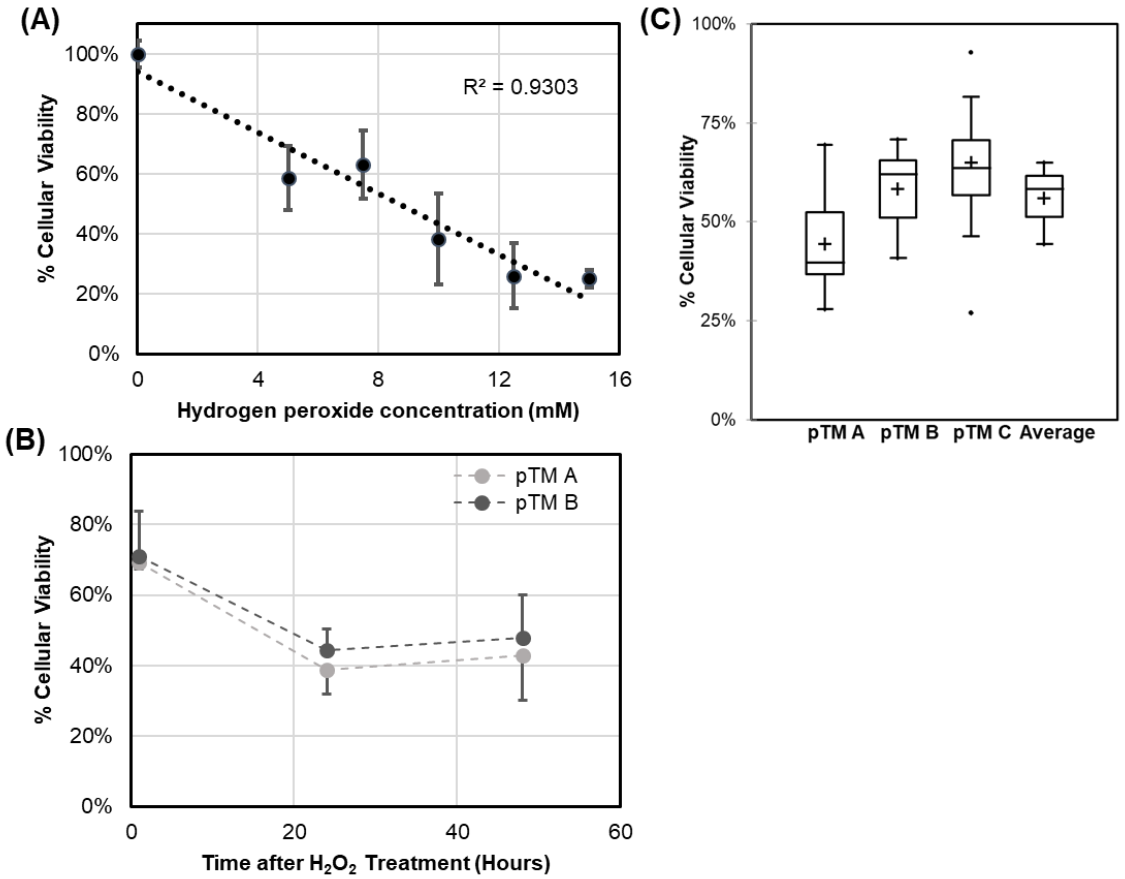

Figure 3. *In Vitro* Effects of Hydrogen Peroxide on pTM Cells. (A) Effect of H_2O_2 concentration on pTM cellular viability immediately following 1-hour treatment (n = 4 technical replicates). (B) Prolonged effects of 1-hour, 2mM H_2O_2 treatment on pTM cellular viability (n = 12 technical replicates). (C) Effects of 1-hour, 2mM H_2O_2 treatment followed by a 24-hour stabilization period on three pTM cell lines (n = 12 technical replicates). Error bars denote standard deviation. All cellular viability values were normalized to untreated, control values.

3.2 Effect of Hydrogen Peroxide on pTM Cell Function

Functional assessments of pTM cells *in vitro* was performed after 2mM H_2O_2 treatment for 1 hour followed by incubation in serum-free media for 24 hours. Metabolic activity, evaluated by an Alamar Blue assay, was significantly reduced following H_2O_2 treatment (Figure 4a). There was a slight decrease in phagocytic activity after incubation with pHrodo *e. coli* particles, however, average differences were not significant (Figure 3b). For all pTM cell lines tested, H_2O_2 treated cells showed insignificant changes in cellular contractility compared to untreated, control pTM cells (Figure 3c). We conclude that H_2O_2 treatment reduces the metabolic activity of pTM cells without altering their phagocytic or contractile responses (Snider, 2018).

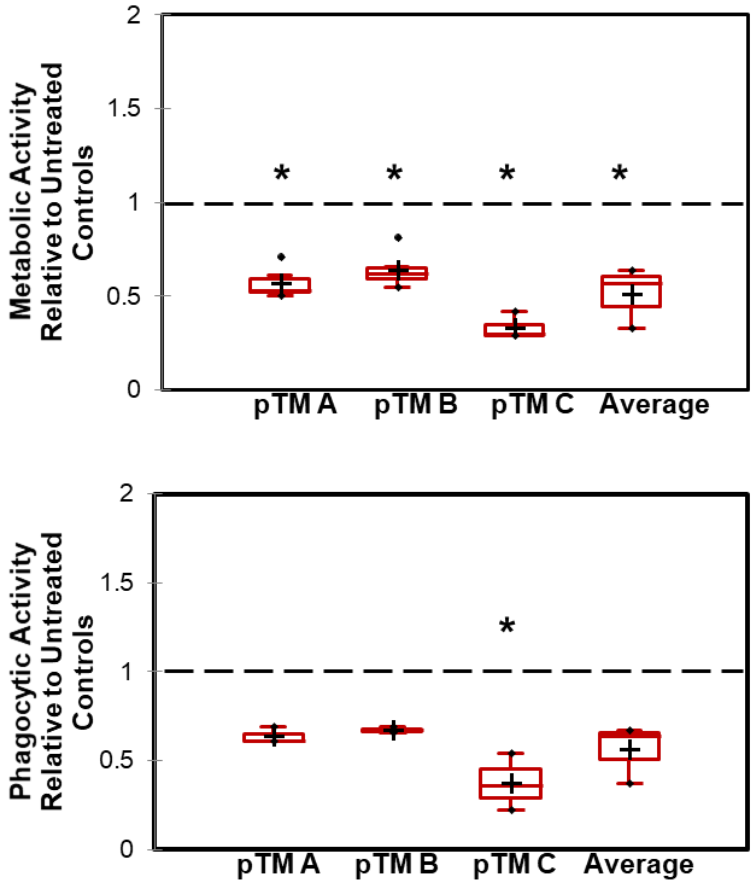

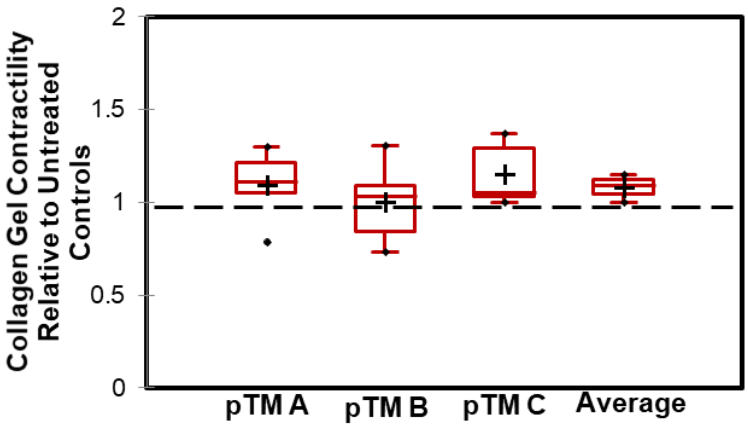

Figure 3. Functional Assessment of Hydrogen Peroxide Treated pTM Cells. pTM cells were treated with 2mM H_2O_2 for 1 hour, then returned to serum-free media. After 24 hours, assessments were performed on pTM cellular (A) metabolic activity (n = 6 technical replicates), (B) phagocytic activity (n = 3 technical replicates), and (C) collagen gel contractility (n = 6 technical replicates). Dashed lines represent the results of untreated, control pTM cells and error bars denote standard deviation. Significant differences between H_2O_2 treated cells and untreated, controls were determined by ANOVA, post hoc Tukey ($p < 0.05$) and are denoted by asterisks.

3.3 Effect of Hydrogen Peroxide on Organ Culture IOP Homeostasis

Following *in vitro* H_2O_2 experiments with pTM cells, experiments were translated to porcine anterior segment organ culture eyes. Different concentrations of H_2O_2 were perfused for 1 hour followed by a 24-hour stabilization period. After IOP stabilization the perfusion flow rate was doubled with the 2x flow challenge for 72 hours to determine the ability of the intact TM to adapt to the increased pressure. Although 2mmM H_2O_2 had a significant effect for *in vitro* experiments, 2-4mM H_2O_2 did not cause significant TM dysfunction and IOP returned to baseline levels (data not shown). A 4.5mM H_2O_2 treatment concentration however, resulted in sustained IOP elevation for at least 3 days following the introduction of 2x flow (Figure 4a). Steady-state IOPs of H_2O_2 treated organ culture eyes following the 2x flow challenge were significantly increased compared to the IOPs of untreated, control eyes (Figure 4b) and we conclude that 4.5mM H_2O_2 treatment creates porcine TM dysfunction that leads to dysregulation of IOP (Snider, 2018).

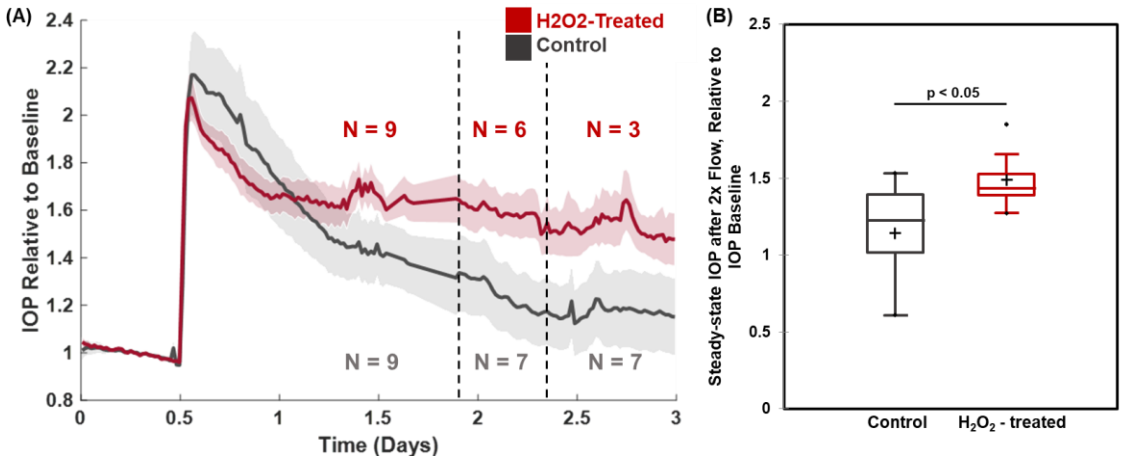

Figure 4. IOP stabilization during 2x Perfusion Flow Challenge Following Hydrogen Peroxide Treatment. IOP was normalized to an eye-specific baseline measured after treatment with H_2O_2 (experimental) or media (control) and before the start of the 2x flow challenge. (A) Average IOP traces for H_2O_2 treated and untreated, control organ culture eyes throughout the 2x flow challenge. Shaded regions denote standard error and N values indicate the number of eyes at each time point. (B) Steady-state IOP after the 2x flow challenge for H_2O_2 treated and untreated, control eyes (n = 9 for each group). Significant differences between groups were determined by ANOVA, post hoc Tukey ($p < 0.05$) and are denoted by asterisks.

3.4 Live-Dead Assessment of Organ Culture TM After Hydrogen Peroxide Treatment

Porcine organ culture tissue was assessed 24 hours after H_2O_2 treatment for TM cellular viability. Staining with calcein-AM (live) and ethidium homodimer-1 (dead) revealed decreased live and increased dead signal in the TM region for H_2O_2 treated anterior segments compared to untreated, control eyes (Figures 5a and 5b). The effects on viability were not uniform across the entire TM region, likely due to the segmental nature of TM outflow (Chang et al., 2014; Swaminathan et al., 2014). Live to dead fluorescent signal ratios were calculated for the entire TM region and the cornea. H_2O_2 treated eyes consistently exhibited lower live-dead ratios; however, the differences to untreated, control eyes were not significant (Figure 5c).

Inconsistencies with dead staining were apparent in many of the tissue sections, with some regions of the TM negative for both ethidium homodimer-1 and calcein-AM. Oxidative stress is known to cause the destruction of nuclear DNA and as ethidium homodimer-1 is a nuclear dead stain, minimal dead staining is possible even with reduced cellular viability (Das et al., 2001; Liu et al., 2013; Nandi et al., 2010; Teramoto et al., 1999). To address potential dead staining inconsistencies, live fluorescent signal intensities were directly compared (5d). A

significant reduction in live signal intensity in the TM region of H_2O_2 treated eyes was observed while the reduction in live staining in the cornea was not statistically significant (Snider, 2018).

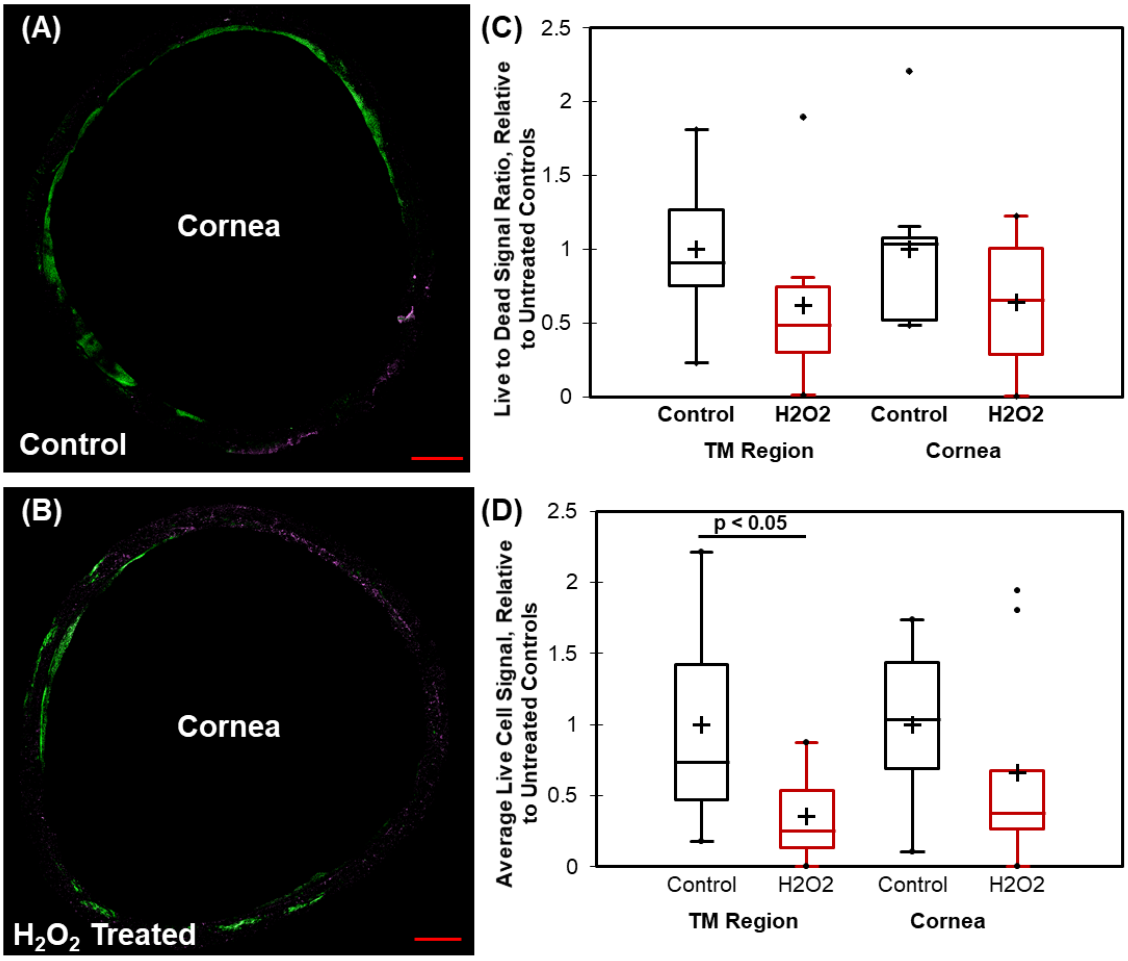

Figure 5. Live-Dead Staining of Porcine Anterior Segment Organ Culture Tissue. Representative *en face* images for the TM region of (A) untreated, control and (B) H_2O_2 treated eyes. Calcein-AM (green) and Ethidium homodimer-1 (red) represent live and dead cells, respectively. Scale bars are 2mm. (C-D) Quantification of Live and Dead fluorescent intensities in the TM region and cornea for H_2O_2 treated and untreated, control organ culture eyes (n = 9 for each group), relative to control values. (C) Live to dead fluorescent intensity ratios and (D) Live fluorescent signal intensities are shown. Significant differences between H_2O_2 treated and untreated, control eyes were determined by ANOVA, post hoc Tukey ($p < 0.05$) and are denoted by asterisks.

4 DISCUSSION

The elevated IOP and optic nerve head damage characteristic of glaucoma is thought to be caused by tissue dysfunction and increased outflow resistance resulting from reduced TM cellularity. This study demonstrates that porcine anterior chamber organ culture can be used to accurately model TM dysfunction in glaucoma.

4.1 In Vitro pTM Cell Characterization

In culture, H_2O_2 treatment of pTM cells resulted in decreased cell viability in a dose-dependent manner. Interestingly, the effects of H_2O_2 were not fully realized until 24 hours after treatment suggesting that cell death may be due to apoptosis (de Bono & Yang, 1995). Metabolic activity was markedly reduced in surviving cells following H_2O_2 treatment; however, phagocytic ability and contractile function were not significantly altered. This aligns with clinical observations in glaucoma, where the remaining TM cells appear to maintain phagocytic activity despite the overall loss of cellularity (Matsumoto & Johnson, 1997).

4.2 Porcine Anterior Chamber Organ Culture Glaucoma Model

Porcine organ cultured eyes showed a significant reduction in cellularity after H_2O_2 treatment, as determined by live-dead staining. For glaucomatous human tissue, roughly 30% fewer cells are found in the TM of POAG donors compared to age-matched healthy controls (Alvarado et al., 1984; Liton et al., 2005). Factoring in an approximately 60% reduction in TM cellularity associated with aging to 80 years, we estimate that there are 70-80% fewer TM cells in aged glaucoma eyes compared to young, healthy tissue (Snider, 2018). Following 4.5mM H_2O_2 exposure for 1 hour, the viability of treated pTM cells in tissue samples was approximately 35% of that in untreated, control eyes. Assuming the control eyes are from young, healthy pigs, this 35% viability, or 65% fewer cells, is close to the reduction in cellularity seen in glaucoma.

Organ culture H_2O_2 concentration was determined by the loss of IOP homeostasis rather than a percentage decrease in pTM cellularity. Untreated, control eyes recovered to baseline IOP levels after 48 hours whereas H_2O_2 treated eyes remained at elevated IOP. This loss of IOP homeostasis provides functional evidence that oxidative stress through H_2O_2 treatment is capable of effecting TM function. Remarkably, loss of IOP homeostasis corresponded to a reduction in TM cellularity similar to that observed in human glaucomatous tissue (Snider, 2018).

5 CONCLUSIONS

The porcine anterior chamber organ culture model with oxidative stress induced TM dysfunction described in this study is an improved platform for studying regenerative medicine therapies for restoring cellularity and functionality to the TM in glaucoma. Porcine eyes are similar in size to humans, making it likely that findings from this model will be easily translatable to human eyes. Organ culture pTM cellularity was reduced to near glaucomatous levels after H_2O_2 treatment and loss of IOP homeostasis, presumably due to reduced tissue remodeling ability, was observed after artificial pressure elevation.

Damage from H_2O_2 is non-specific and other anterior chamber tissues may also exhibit reduced cellularity, potentially introducing confounding factors when testing cell therapies. The non-specificity of the treatment also means that this approach is likely not suitable for *in vivo* applications. Future steps will involve increasing the specificity of the H_2O_2 treatment and beginning to test mesenchymal stem cell (MSC) therapies with the organ culture model to determine their capacity for restoring TM cellularity and function.

REFERENCES

Abu-Hassan, D. W., Li, X., Ryan, E. I., Acott, T. S., & Kelley, M. J. (2015). Induced pluripotent stem cells restore function in a human cell loss model of open-angle glaucoma. *Stem Cells (Dayton, Ohio), 33*(3), 751-761. doi:10.1002/stem.1885

Acott, T. S., & Kelley, M. J. (2008). Extracellular matrix in the trabecular meshwork. *Experimental Eye Research, 86*(4), 543-561. doi:10.1016/j.exer.2008.01.013

Acott, T. S., Kelley, M. J., Keller, K. E., Vranka, J. A., Abu-Hassan, D. W., Li, X., . . . Bradley, J. M. (2014). Intraocular pressure homeostasis: maintaining balance in a high-pressure environment. *Journal Of Ocular Pharmacology And Therapeutics: The Official Journal Of The Association For Ocular Pharmacology And Therapeutics, 30*(2-3), 94-101. doi:10.1089/jop.2013.0185

Alvarado, J., Murphy, C., & Juster, R. (1984). Trabecular meshwork cellularity in primary open-angle glaucoma and nonglaucomatous normals. *Ophthalmology, 91*(6), 564-579.

Alvarado, J., Murphy, C., Polansky, J., & Juster, R. (1981). Age-related changes in trabecular meshwork cellularity. *Investigative Ophthalmology & Visual Science, 21*(5), 714-727.

Bachmann, B., Birke, M., Kook, D., Eichhorn, M., & Lütjen-Drecoll, E. (2006). Ultrastructural and biochemical evaluation of the porcine anterior chamber perfusion model. *Investigative Ophthalmology & Visual Science, 47*(5), 2011-2020.

Bhattacharya, S. K., Gabelt, B. A. T., Ruiz, J., Picciani, R., & Kaufman, P. L. (2009). Cochlin expression in anterior segment organ culture models after TGFbeta2 treatment. *Investigative Ophthalmology & Visual Science, 50*(2), 551-559. doi:10.1167/iovs.08-2632

Brubaker, R. F. (1970). The measurement of pseudofacility and true facility by constant pressure perfusion in the normal rhesus monkey eye. *Investigative Ophthalmology, 9*(1), 42-52.

Brubaker, R. F. (1991). Flow of aqueous humor in humans [The Friedenwald Lecture]. *Investigative Ophthalmology & Visual Science, 32*(13), 3145-3166.

Buller, C., Johnson, D. H., & Tschumper, R. C. (1990). Human trabecular meshwork phagocytosis. Observations in an organ culture system. *Investigative Ophthalmology & Visual Science, 31*(10), 2156-2163.

Chang, J. Y. H., Folz, S. J., Laryea, S. N., & Overby, D. R. (2014). Multi-scale analysis of segmental outflow patterns in human trabecular meshwork with changing intraocular

pressure. *Journal of Ocular Pharmacology and Therapeutics, 30*(2-3), 213-223. doi:10.1089/jop.2013.0182

Clopton, D. A., & Saltman, P. (1995). Low-level oxidative stress causes cell-cycle specific arrest in cultured cells. *Biochemical And Biophysical Research Communications, 210*(1), 189-196.

Das, M., Mukherjee, S. B., & Shaha, C. (2001). Hydrogen peroxide induces apoptosis-like death in Leishmania donovani promastigotes. *Journal of Cell Science, 114*(13), 2461.

de Bono, D. P., & Yang, W. D. (1995). Exposure to low concentrations of hydrogen peroxide causes delayed endothelial cell death and inhibits proliferation of surviving cells. *Atherosclerosis, 114*(2), 235-245. doi:https://doi.org/10.1016/0021-9150(94)05488-5

Dismuke, W. M., Liang, J., Overby, D. R., & Stamer, W. D. (2014). Concentration-related effects of nitric oxide and endothelin-1 on human trabecular meshwork cell contractility. *Experimental Eye Research, 120*, 28-35. doi:10.1016/j.exer.2013.12.012

Erickson-Lamy, K., Rohen, J. W., & Grant, W. M. (1991). Outflow facility studies in the perfused human ocular anterior segment. *Experimental Eye Research, 52*(6), 723-731.

Gaasterland, D., & Kupfer, C. (1974). Experimental glaucoma in the rhesus monkey. *Investigative Ophthalmology, 13*(6), 455-457.

Gagen, D., Filla, M. S., Clark, R., Liton, P., & Peters, D. M. (2013). Activated αvβ3 integrin regulates αvβ5 integrin-mediated phagocytosis in trabecular meshwork cells. *Investigative Ophthalmology & Visual Science, 54*(7), 5000-5011. doi:10.1167/iovs.13-12084

Grierson, I., & Howes, R. C. (1987). Age-related depletion of the cell population in the human trabecular meshwork. *Eye (London, England), 1 (Pt 2)*, 204-210.

Ishikawa, M., Yoshitomi, T., Zorumski, C. F., & Izumi, Y. (2015). Experimentally induced mammalian models of glaucoma. *Biomed Research International, 2015*, 281214-281214. doi:10.1155/2015/281214

Izzotti, A., Saccà, S. C., Longobardi, M., & Cartiglia, C. (2009). Sensitivity of ocular anterior chamber tissues to oxidative damage and its relevance to the pathogenesis of glaucoma. *Investigative Ophthalmology & Visual Science, 50*(11), 5251-5258. doi:10.1167/iovs.09-3871

Johnson, D. H., & Tschumper, R. C. (1987). Human trabecular meshwork organ culture. A new method. *Investigative Ophthalmology & Visual Science, 28*(6), 945-953.

Johnson, D. H., & Tschumper, R. C. (1989). The effect of organ culture on human trabecular meshwork. *Experimental Eye Research, 49*(1), 113-127.

Knepper, P. A., Goossens, W., & Palmberg, P. F. (1996). Glycosaminoglycan stratification of the juxtacanalicular tissue in normal and primary open-angle glaucoma. *Investigative Ophthalmology & Visual Science, 37*(12), 2414-2425.

Liton, P. B., Challa, P., Stinnett, S., Luna, C., Epstein, D. L., & Gonzalez, P. (2005). Cellular senescence in the glaucomatous outflow pathway. *Experimental Gerontology, 40*(8-9), 745-748.

Liu, J., Wang, Y., Du, W., Liu, W., Liu, F., Zhang, L., . . . Yu, B. (2013). Wnt1 inhibits hydrogen peroxide-induced apoptosis in mouse cardiac stem cells. *PLOS ONE, 8*(3), e58883. doi:10.1371/journal.pone.0058883

Mao, W., Tovar-Vidales, T., Yorio, T., Wordinger, R. J., & Clark, A. F. (2011). Perfusion-cultured bovine anterior segments as an ex vivo model for studying glucocorticoid-induced ocular hypertension and glaucoma. *Investigative Ophthalmology & Visual Science, 52*(11), 8068-8075. doi:10.1167/iovs.11-8133

Matsumoto, Y., & Johnson, D. H. (1997). Trabecular meshwork phagocytosis in glaucomatous eyes. *Ophthalmologica. Journal International D'ophtalmologie. International Journal Of Ophthalmology. Zeitschrift Fur Augenheilkunde, 211*(3), 147-152.

Morrison, J. C., Moore, C. G., Deppmeier, L. M., Gold, B. G., Meshul, C. K., & Johnson, E. C. (1997). A rat model of chronic pressure-induced optic nerve damage. *Experimental Eye Research, 64*(1), 85-96.

Nandi, N., Sen, A., Banerjee, R., Kumar, S., Kumar, V., Ghosh, A. N., & Das, P. (2010). Hydrogen peroxide induces apoptosis-like death in Entamoeba histolytica trophozoites. *Microbiology, 156*(7), 1926-1941. doi:doi:10.1099/mic.0.034066-0

O'Brien, J., Wilson, I., Orton, T., & Pognan, F. (2000). Investigation of the Alamar Blue (resazurin) fluorescent dye for the assessment of mammalian cell cytotoxicity. *European Journal Of Biochemistry, 267*(17), 5421-5426.

Quigley, H. A., & Broman, A. T. (2006). The number of people with glaucoma worldwide in 2010 and 2020. *The British Journal Of Ophthalmology, 90*(3), 262-267.

Saccà, S. C., Pascotto, A., Camicione, P., Capris, P., & Izzotti, A. (2005). Oxidative DNA damage in the human trabecular meshwork: clinical correlation in patients with primary open-angle glaucoma. *Archives Of Ophthalmology (Chicago, Ill.: 1960), 123*(4), 458-463.

Senatorov, V., Malyukova, I., Fariss, R., Wawrousek, E. F., Swaminathan, S., Sharan, S. K., & Tomarev, S. (2006). Expression of mutated mouse myocilin induces open-angle glaucoma in transgenic mice. *The Journal Of Neuroscience: The Official Journal Of The Society For Neuroscience, 26*(46), 11903-11914.

Shareef, S. R., Garcia-Valenzuela, E., Salierno, A., Walsh, J., & Sharma, S. C. (1995). Chronic ocular hypertension following episcleral venous occlusion in rats. *Experimental Eye Research, 61*(3), 379-382.

Sherwood, M. E., & Richardson, T. M. (1988). Phagocytosis by trabecular meshwork cells: sequence of events in cats and monkeys. *Experimental Eye Research, 46*(6), 881-895.

Snider, E. (2018). *Mesenchymal stem cell therapies for the trabecular meshwork in glaucoma.* (Doctor of Philosophy Dissertation), Georgia Institute of Technology and Emory University,

Snider, E., Vannatta, R. T., Schildmeyer, L., Stamer, W. D., & Ethier, C. R. (2018). Characterizing differences between MSCs and TM cells: Toward autologous stem cell therapies for the glaucomatous trabecular meshwork. *Journal Of Tissue Engineering And Regenerative Medicine, 12*(3), 695-704. doi:10.1002/term.2488

Stamer, W. D., Seftor, R. E., Williams, S. K., Samaha, H. A., & Snyder, R. W. (1995). Isolation and culture of human trabecular meshwork cells by extracellular matrix digestion. *Current Eye Research, 14*(7), 611-617.

Swaminathan, S. S., Oh, D.-J., Kang, M. H., & Rhee, D. J. (2014). Aqueous outflow: segmental and distal flow. *Journal of cataract and refractive surgery, 40*(8), 1263-1272. doi:10.1016/j.jcrs.2014.06.020

Tamm, E. R. (2002). Myocilin and glaucoma: facts and ideas. *Progress In Retinal And Eye Research, 21*(4), 395-428.

Tanito, M., Kaidzu, S., Takai, Y., & Ohira, A. (2016). Association between systemic oxidative stress and visual field damage in open-angle glaucoma. *Scientific Reports, 6*, 25792-25792. doi:10.1038/srep25792

Teramoto, S., Tomita, T., Matsui, H., Ohga, E., Matsuse, T., & Ouchi, Y. (1999). Hydrogen peroxide-induced apoptosis and necrosis in human lung fibroblasts: Protective roles of glutathione. *The Japanese Journal of Pharmacology, 79*(1), 33-40. doi:10.1254/jjp.79.33

Weber, A. J., & Zelenak, D. (2001). Experimental glaucoma in the primate induced by latex microspheres. *Journal Of Neuroscience Methods, 111*(1), 39-48.

Weih, L. M., Nanjan, M., McCarty, C. A., & Taylor, H. R. (2001). Prevalence and predictors of open-angle glaucoma: Results from the visual impairment project. *Ophthalmology, 108*(11), 1966-1972. doi:https://doi.org/10.1016/S0161-6420(01)00799-0

Weinreb, R. N., Aung, T., & Medeiros, F. A. (2014). The pathophysiology and treatment of glaucoma: a review. *JAMA, 311*(18), 1901-1911. doi:10.1001/jama.2014.3192

Yu, A. L., Fuchshofer, R., Kampik, A., & Welge-Lüssen, U. (2008). Effects of oxidative stress in trabecular meshwork cells are reduced by prostaglandin analogues. *Investigative Ophthalmology & Visual Science, 49*(11), 4872-4880. doi:10.1167/iovs.07-0984

Zhang, Z., Dhaliwal, A. S., Tseng, H., Kim, J. D., Schuman, J. S., Weinreb, R. N., & Loewen, N. A. (2014). Outflow tract ablation using a conditionally cytotoxic feline immunodeficiency viral vector. *Investigative Ophthalmology & Visual Science, 55*(2), 935-940. doi:10.1167/iovs.13-12890

Zhao, J., Wang, S., Zhong, W., Yang, B., Sun, L., & Zheng, Y. (2016). Oxidative stress in the trabecular meshwork (Review). *International Journal Of Molecular Medicine, 38*(4), 995-1002. doi:10.3892/ijmm.2016.2714